



# WEAR AND CRYSTALLIZATION BEHAVIOR OF A GRAY CAST IRON SURFACE TREATMENT BY SULPHUR ADDITIONS IN THE MOULDING SAND

*Gamal E.Y. Abouraya<sup>1</sup>, Mohamed M. Abdalla<sup>2</sup>*

<sup>1</sup>: Faculty of Engineering, Port Said University, EGYPT.

<sup>2</sup>: Faculty of Engineering, Omar Almuhttar University, Elbeida, LIBYA.

## ABSTRACT

The aim of this paper is to study the surface treatments of grey cast iron by sulphur additions into a face moulding sand on the microstructure, hardness and wear resistance of the skin layer of casting. To evaluate the wear behavior a Pin-on-Disk wear test machine was used. Pins which were prepared from the samples with the skin layer treatment by different sulphur additions of 0, 1, 2,4, 6, 8, 10 wt.% on the face moulding sand were worn on a steel counterface having a hardness of 63HRC under applied load of 80 N at a constant sliding velocity of 1200 rpm.

Results showed that sulphur lead to white iron skin layer formation and the thickness of which is depended either on both sulphur content and casting wall thickness (cooling rate). An increase of casting thickness ranging from 10 up to 40 mm increased the thickness of white cast iron as well. These both factors mentioned above influenced the microstructure of white iron layer, which changed from hypoeutectic to hypereutectic in mode.

The wear and hardness results indicate that the surface treatment grey cast iron exhibits superior wear properties and have high hardness to as cast gray cast iron under the similar conditions. Therefore, this hard layer caused by the formation of a microstructure martensite and cementite phases resulted in a better wear resistance in comparison to the as cast samples. Higher sulphur content result in greater pearlite and cementite (ledeburite) contents and hardness. Both sulfur and casting thicknesses increase the amount of ledeburite formed in skin layer casting throw the transformation range. For casting of thickness 40 mm and sulphur content 10 wt.%, was characterized with coarse lath of primary  $Fe_3C$  precipitate in ledeburitic matrix. The grey iron casting surface treatment with 6% sulphur added into the face molding sand exhibits the best wear resistance, hardness and clear white iron microstructure in the skin layer.

**KEY WORDS:** White cast iron; Surface layer; Sulphur; Wear.

## 1. INTRODUCTION

Gray cast iron is an inexpensive and really available material and its specific characteristics such as low melting point, excellent castability along with no freezing contraction have given it decent capability for fabrication of complicated components by using the simplest and most economic methods[1-3]. Graphite flakes are interacted together and disposed in the form of plates, constituting an easy path for fast heat dissipation, good ability for vibration damping and excellent machinability[4]. These properties mainly make gray cast iron as a desirable option for fabrication of the parts which are in the exposure to the repeated local thermal stresses.

Gray cast iron with pearlitic matrix can damp vibration more efficiently than ferritic or martensitic matrix and also it has better performance than ferritic gray cast iron due to their better mechanical properties[7-8]. Despite favorable characteristics of gray cast iron, sharp edge of flake graphites contributes to stress concentration and crack formation[9].

This undesirable character resulted from the graphite morphology can also deteriorate the wear resistance of this type of cast iron under shear stresses applied during a dry sliding wear specially at high applied loads. Hence, to benefit from this inexpensive cast iron in the wear applications, their surface can be modified by using surface engineering techniques[10-11].

Recent research efforts have been concentrated on the development of surface layers of gray cast iron with improved properties[12-13]. Surface melting is a process in which the surface of the workpiece is melted and resolidified when being exposed to a high power beam such as laser or electron beam. The surface melted layer has usually a finer and more homogeneous structure than its original base material [14]. Increase in solid solubility and creation of metastable crystalline phases in the melted region can also occur. So it seems to be appreciable to concentrate more on this process in surface modification and effect of its variations on wear behavior of the cast iron in detail[15]. Surface hardening is an important aspect of the heat treatment of cast iron. In applications requiring resistance to wear and abrasion, exceptionally hard surfaces can be obtained on cast iron

by heating into austenitic range followed by cooling. Control of this process leads to control of the transformation product phases and to variation in hardness and mechanical behavior. Recent interest has been centered on glazing of cast iron surfaces[16].

Many authors have shown that sulphur play a significant role in the process of crystallization of cast iron and nevertheless it is thought as an impurity[17]. Sulphur chemically acts to stabilize iron carbide, although it does not participate in the carbide formation. It has a very strong influence; it is ordinarily considered that each 0.01% S is sufficient to neutralize the graphitizing influence of 0.15% Si. Amount of sulphur dissolved in austenite and cementite. It concentrates at the eutectic cells grain boundaries and in graphite precipitations. The information in publication on the influence of sulphur on crystallization and the structure of cast iron refers to relatively small sulphur contents [18].

However, sulphur has strong affinity for manganese sulfide compound (MnS) which has little influence on carbide or graphite formation[19]. The effect of both sulphur and manganese alone in cast irons is to restrict graphitization and promote pearlite formation. Thus, either sulphur or manganese alone in cast irons is carbide-stabilizing element[19]. Therefore, the first additions of sulphur to an iron with a moderately high manganese content have an indirect graphitization tendency to removing the carbide-stabilizing manganese to a moderately high-sulphur iron remove some of the sulphur from an active to inactive role and thus promote graphitization. Sulphur inhibits graphitization and helps to produce a hard, brittle white iron. Moreover, its produce as the sulfide (FeS) in cast iron will also increase the tendency to brittleness. On the other hand the high concentrations of sulphur promote the crystallization in the metastable Fe-Fe<sub>3</sub>C system[20].

In the present paper, an attempt has been made to investigate the effects of surface treatments of gray cast iron by sulphur added into the moulding sand in surface modification and effect of its variation on wear behavior of the gray cast iron in detail. In this study improvement of wear resistance of the gray cast iron by sulphur added to the moulding sand are evaluated. Dry sliding wear are carried out using a pin-on-disc wear testing machine. Brinll hardness were measured on the surface treatment by sulphur of the samples. The experiment sulphur was simply an additive to the sand mix and its role was to create a hard and wear resistance white iron skin layer on the gray castings.

## 2. EXPERIMENTAL METHODS

### 2.1 Specimen Preparation and Microstructural Examination

The melt utilized in the present study were produced by using a 50 Kg medium frequency induction furnace in Suez Canal Shipyard of Port Said. Chemical composition

of cast iron samples were controlled ; 3.11 wt.% C, 1.59 wt.% Si, 0.32 wt.% Mn, 0.08 wt.% S, 0.02 wt.% P and remainder Fe. Before pouring, liquid metal was inoculated with FeSi<sub>75</sub> alloy. The samples were a stair shape castings of thickness 10 mm, 20 mm, 30 mm, and 40mm, wide 40mm and 600mm long. The samples were prepared in the moulding sand with a different amount of sulphur mixed with a facing sand. The facing sand was produced by mixing sulphur powder in the sand in mixing machine with mixing time not less than 15 min. The face moulding mixture was green sand mould, which contained; 9 wt% bentonite, 5 wt% water, and silica sand. The additions of sulphur were 0, 1, 2, 4, 6, 8, and 10 wt% of the face moulding sand. The pouring temperature was kept to be 1380°C. The melt temperature was always checked in the pouring ladle before pouring by means of an immersion thermocouple.

After the castings were cooled to room temperature, it were split up. The specimens of metallograpy were cut exactly from the same place of each casting in rectangular shape. The specimens were prepared by traditionally mechanical grinding and polishing of the surface located in a plane perpendicular to the treatment skin layer. The surface of the specimen was held lightly on a horizontally rotating polishing disc covered with "Selvyt" cloth. Liquid abrasive compound and polishing agents, diamond dust were applied to the selvyt cloth while the specimens were being polished. After polishing, the specimens were immersed and swabbed in the etching 2%-4% nital solution for 10 to 20 sec. When etching is complete, the specimens is rinsed in running water and then in alcohol and dry using a stream of warm air. The polished and etched specimens were inspected in the optical microscope of type "Nikon".

The specimens for scanning electron microscopy (SEM) observations were prepared from white iron layer obtained in two casting of thickness 10 mm. These specimens were taken from the same part from the casting obtained in the mould with 2% and 8 wt % sulphur to reveal some details of skin layer morphology.

The hardness measurements were carried out on the polished samples with 0, 1, 2, 4, 6, 8, and 10% wt. sulphur added into the molding sand. The Brinll testes were preformed on the universal testing machine using a constant load of 3000 kg applied on a 10 mm ball diameter with time of loading recommended is 20 sec for gray cast iron specimen in Materials Science Lab in Faculty of Engineering at Port Said University. An average of three observations has been considered in this study.

### 2.2 Wear Test

The sliding wear test was performed on 10 mm diameter, and 40 mm long cylindrical pin samples that were machined from gray iron surface treatment castings. A pin-on-disc machine shown in Figure 1 was used for wear testing with a constant load of 80 N and rotating speed of 1200 rpm and a constant area of the samples. The disc was fabricated using a steel having

hardness 63HRC after heat treatment. The specimen and disc surfaces were grinded and polished prior to starting the tests. Cleaning of the disc and pin samples was done using water followed by ethanol alcohol. Wear loss were measured by a weight loss technique. The samples were weighed prior to and after wear testing using a Mettler microbalance having a precision level of 0.01 mg. An average of three observations has been considered in this study.

### 3. RESULTS AND DISCUSSIONS

#### 3.1. Morphology

Figure 2 shows the microstructure of the grey cast iron with 0 wt.% sulphur in the moulding sand. The microstructure is showed a flak graphite with uniform distribution and random orientation in a matrix of ferrite (type A). The ferritic matrix is relatively weak in cast iron which has a relatively low strength and the hardness. The graphite flakes have a weakening effect on strength by acting like notches.

Microstructure of gray irons surface with 1 wt.% sulphur added into the molding sand are shown in Fig. 3 (a:d) with different cooling rate of thicknesses 10 mm, 20 mm, 30 mm, and 40 mm thickness. The photos illustrates a white iron structure typical for hypoeutectic cast iron. The structure is revealed a long dendrites of primary austenite, transformed into pearlite during eutectoidal transformation as shows in Fig. 3a. In many cases these dendrites lie along the direction of maximum heat transfer. The pictures have essentially white cast iron for high cooling rate fine dendritic of pearlite and interdendritic carbide and for slow cooling rate showing coarse dendritic pattern of pearlite and interdendritic carbide are shown in Fig. 3 (b:d) . The white constituent is iron carbide and the grey areas are unresolved pearlite.

Figures 4 (a:b) show the microstructures of skin layer of the specimens with 2 % wt. sulphur as a function of casting thickness (with different cooling rate). The white cast iron has a fine dendritic of pearlite and interdendritic iron carbide of high cooling rate as shown in Fig. 4a and 4b. When the cooling rate is slow the specimen has a coarse dendritic of pearlite and interdendritic iron carbide as shown in Fig. 4d. The white iron showing a dendritic pattern of fine pearlite (dark area), and an interdendritic mixture of massive and acicular free cementite (light) with some pearlite. More detailed metallographic observation, carried out on scanning electron at higher magnification in Fig. 5 a and b showed a MnS precipitates, located at the interface between carbide and pearlite structure.

Figures 6 (a:d) illustrate the microstructure of casting specimens obtained in the mould containing 4 % wt. of sulphur as function of casting thicknesses (different cooling rates). It is easy to see that even through all of them are white iron skin layers they differ each from the other with different thickness and cooling rates. White iron showing interdendritic network of carbide and large dendritic of pearlite with lath morphology cementite

growing inside them. In Fig. 6 (a:d) the dark areas is pearlite (too fine to be resolved at the magnification employed) and the white areas are cementite.

Figures 7 (a:d) show the microstructures of skin layer of the specimens with 6% wt. sulphur added into the molding sand with different cooling rates and thicknesses 10 mm, 20 mm, 30 mm, and 40 mm. The photographs are shown mixed white cast iron with pearlite and cementite and partially ledeburitic as shown in Fig. 7d.

Figures 8 (a:d) show the microstructure of the specimens with 8% wt. sulphur added to the molding sand with different cooling rates and thicknesses of 10 mm, 20 mm, 30 mm and 40 mm. The microstructures are very similar to the microstructure of eutectic white iron which is ledeburitic in mode, however it is fully ledeburitic white iron structures. Fig. 9 shows the scanning electron micrograph specimen with 8% wt. sulphur for thickness  $t = 10$  mm at 2000X. The micrograph shows a primary  $Fe_3C$  are clear visible and a lamellar pearlite.

Figures 10 (a:d) show the microstructure of the specimens with 10% wt. sulphur added inside the moulding sand with different cooling rates and thickness 10, 20, 30 and 40 mm respectively . In these structures thin, needle-like primary  $Fe_3C$  precipitates are observed, indicating the hypereutectic type of solidification process. The effect of the cooling rates on the structure are clearly shown. The main feature of that white iron skin layer is more coarse microstructure for slow cooling rates ( see Figures 8c and 8d ). It is easy to see, that even though all of them are white iron skin layers, and they differ each from other. More detailed metallographic observations carried out at higher magnification showed no sulphur manganese precipitates inside whit iron skin layer as shown in Fig. 5 and Fig. 9.

#### 3.2. Results of Hardness Test

Figure 11 shows the results of the Brinel hardness tests of the specimens as a function of sulphur additions into the face moulding sand for the casting thickness of 10 mm, 20 mm, 30 mm, and 40mm . As shown in Figure 11 the surface treatment by sulphur additions exhibited high hardness than the specimens without treatments. It can be also seen that by increasing the sulphur, the hardness of the samples increased drastically for all thickness, especially at 10 wt% sulphur.

For thickness 10 mm, the hardness increases with increasing the sulphur addition on the molding sand from 240 to 490  $Kg/m^2$ , and the maximum value of the hardness exist at 10 wt% sulphur. For thickness 20mm, the hardness increases with increasing the sulphur additions on the molding sand from 215 to 510  $kg/mm^2$ , and the maximum value of the hardness exist at 10 wt% sulphur.

For thickness 30 mm, the hardness increases with increasing with increasing the sulphur addition on the moulding sand from 210 to 540  $Kg/mm^2$ , and the

maximum hardness value exist at 10% sulphur. For thickness 40 mm, the hardness increases with increasing the sulphur additions on the moulding sand from 195 to 560 Kg/mm<sup>2</sup>, and the maximum value of hardness exist at 10% sulphur.

The effect of sulphur added into the molding sand in the skin layer of gray cast iron is to restrict the graphitization and promote pearlite formation, thus the sulphur is a carbide stabilizing element. A higher sulphur levels in the molding sand from 1 to 10 wt.% increasing the formation of cementite larger than the constituents. Since cementite is hard and brittle, the increase in the amount of cementite in the skin layer of gray cast iron can increase its hardness and brittleness. It is also decreases the machinability of gray cast iron.

### 3. 3. Results of Wear Test

Fig. 12, 13, 14, 15, 16, 17, 18, 19, 20 and 21 represents the wear loss of the samples with 0, 1, 2, 4, 6, 8, and 10 wt.% sluphur additions as a function of time with a different cooling rate at a constant load 80 N, and the disc rotate at the speed of 1500 rpm.

Figure 12 shows variation of wear loss of the specimen with sulphur 0 wt.% as a function of time and different cooling rate for thickness 10 mm, 20 mm, 30 mm, and 40 mm. The wear loss increasing with increases the time, decreases with the increase of casting thickness, and decreases with the increase of cooling rate. The wear loss changes from 155 to 450 mg.

Fig. 13 shows the wear loss of specimen with 1 wt.% sluphur addition as a function of time with different cooling rate for thickness 10 mm, 20 mm, 30 mm, and 40 mm. The wear loss increases with the increase in time, decreases with the increase in the casting thickness, and decreases with increase of the cooling rate. The wear loss changes from 140 to 435 mg.

Fig. 14 shows the wear loss as a function of time for specimens with 2 wt.% sluphur addition in the molding sand and different cooling rates. The wear loss increases with increasing time, decreases with the increasing of the casting thickness, and decreases with the increase of the cooling rate. The wear loss changes from 135 to 350 mg.

Fig. 15 shows the wear loss as a function of time for specimens with 4 wt.% sluphur addition into the molding sand and different cooling rates. The wear loss increases with increase of time, decreases with the increase of casting thickness, and decreases with the increase of cooling rate. The wear loss changes from 128 to 320 mg.

Fig. 16 shows the wear loss as a function of time for specimens with 6 wt.% sluphur addition into the molding sand and different cooling rates. The wear loss increases with the increase of time, decreases with the increase of the casting thickness, and decreases with the increase of cooling rate. The wear loss changes from 120 to 285 mg.

Fig. 17 shows the wear loss as a function time for specimens with 8% sluphur addition into the molding sand and different cooling rates. The wear loss increases with the increase of time, decreases with the increase of casting thickness, and decreases with the increase of the cooling rate. The wear loss changes from 132 to 205 mg.

Fig. 18 shows the wear loss as a function time for specimens with 10% sluphur addition into the molding sand and different cooling rates. The wear loss increases with the increase of time, decreases with the increase of casting thickness, and decreases with the increase of the cooling rate. The wear loss changes from 65 to 10 mg.

Fig. 19 shows the wear loss as a function of sulphur addition on the molding sand for thickness 10 mm and different wear time of 10, 20, and 30 min. The wear loss decreases with the increase sulphur additions, decreases with the increase of casting thickness, and decreases with increase of the cooling rate.

Fig. 20 shows the wear loss as a function of sulphur addition on the molding sand for thickness 20 mm and different wear time of 10, 20, and 30 min. The wear loss decreases with increase sulphur contents, decreases with increase of casting thickness, and decreases with increase of the cooling rate.

Fig. 21 shows the wear loss as a function of sulphur addition on the molding sand for thickness 30 mm and different wear time 10, 20, and 30min. The wear loss decreases with increase sulphur additions, decreases with the increase of casting thickness, and decreases with the increase of the cooling rate.

Fig. 22 shows the wear loss as a function of sulphur addition on the molding sand for thickness 40 mm and different wear time 10, 20, and 30 min. The wear loss decreases with increase sulphur additions, decreases with the increase of casting thickness, and decreases with the increase of cooling rate.

## 4. CONCLUSIONS

On the basis of the experimental results and discussions, the major conclusions are:

- 1- The sulphur added into the molding sand causes the formation of white iron in skin layer of the specimens of gray cast iron.
- 2- The microstructure of white iron in skin layers of specimens greatly depends on sulphur contents in the molding sand and the cooling rates (the casting thickness).

- 3- The skin layer microstructure of the specimens are hypoeutectic at lower sulphur content and hypereutectic for higher sulphur contents.
- 4- At 10 wt.% sulphur content in sand molding, the microstructure of white cast iron layer changes from eutectic ( $t = 10$  mm) to hypereutectic ( $t = 40$ mm).
- 5- The hardness increases with the increasing of the sulphur added into the molding sand depend on the microstructure transformation.
- 6- The wear resistance of the skin layer of specimens increases with increasing the sulphur addition to the molding sand.
- 7- The skin layer of the specimens with 6% and 8% of sulphur added into the molding sand have an optimum properties of the molding sand, hardness, wear resistance and clearly white cast iron structure.

## REFERENCES

- [1 ] A.W. Orłowicz and A. Trytek: *Wear*, 2003, 254, 154.
- [2 ] A.R. Riahi and A.T. Alpas: *Wear*, 2003, 255, 401-409.
- [3 ] S. Choo, S. Lee and S. Kwon: *Metall. Mater. Trans. A*, 1999, 30A, 1211.
- [4 ] G. Cueva, A. Sinatora, W.L. Guessier and A.P. Tschiptschin: *Wear*, 2003, 255, 1256.
- [5 ] W. Wang, T.F. Jing, Y.W. Gao, G.Y. Qiao and X. Zhao: *J. Mater. Proc. Tech.*, 2007, 182, 593.
- [6 ] *Metals Handbook, Properties and Selection: Irons and Steels*, vol. 1, 9<sup>th</sup>-ed., ASM, Metals Park, Ohio, 1990, 12-40.
- [7 ] E. Takeuchi, *wear*, 19, (1997), 267.
- [8 ] B.K. Prasad: *Mater. Sci. Eng. A*, 2007, 456, 373.
- [9 ] Y. Yamamoto, S. Gondo and N. Tanaka: *Tribol. Lett.*, 2004, 17, 55.
- [10] W.X. Pan, X. Meng, G. Li, Q.X. Fei and C.K. Wu: *Surf. Coat. Tech.*, 2005, 197, 345.
- [11] A.W. Orłowicz and A. Trytek: *Wear*, 2003, 254, 154.
- [12] C.N. Panagopoulos, A.E. Markaki and P.E. Agathocleous: *Mater. Sci. Eng.*, 1998, A241, 226.
- [13] C.C. Koch: *Int. Mater. Rev.*, 1988, 33(4), 201.
- [14] H. Mohamadzadeh, H. Saghafian, and Sh. Kheirandsh, *J. Mater. Sci. Technol.*, Vol. 25 No. 5, 2009, p.p. 622-628.
- [15] D.N.H. Trafford, T. Bell, J.H.P.C. Megaw and A.S. Bransden: *Met. Technol.*, 1983, 10, 69.
- [16] I. Minkoff, "The physical Metallurgy of Cast Iron", John Wiley and Sons Ltd. (1983).
- [16] J.T. Svidro, and Miskolc, *International Foundry Research* 62 (2010) No. 4.
- [17] *Metals Handbook, "Casting"*, vol. 15, 9<sup>th</sup>-ed, ASM, Metals Park Ohio, 1988.
- [18] M. Kaczorowski, and A. Borowski, 1<sup>st</sup> Int. Conf. On Meh. Eng. and Advanced Tech. for Indus. Production, Assiut University, Assiut, EGYPT, Dec. 27-29 1994.
- [19] R.M. Brick, A.W. Pense, and R. B. Grodon, "Structure and Properties of Engineering Materials", McGraw-Hill, Inc., (1977), p.p. 359.
- [20] W.F. Smith, "Structure and Properties of Engineering Alloys", McGraw-Hill Book Company, (1981), p.p. 315-360.

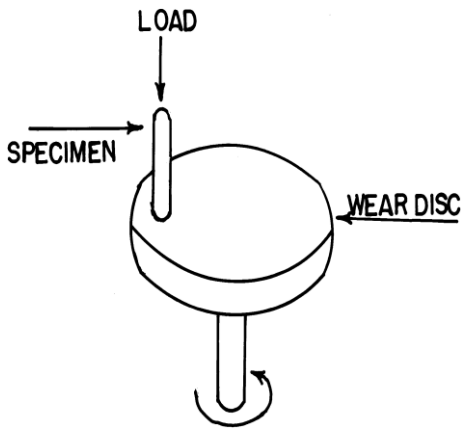


**Fig.1:** A schematic representation of the pin-on-disc machine.

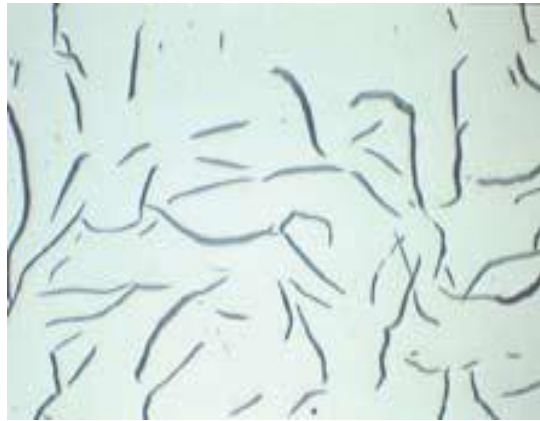


**Fig. 2:** microstructure of gray cast iron of with 0 wt. % sulphur revealing flaky graphite on matrix of ferrite (500X).

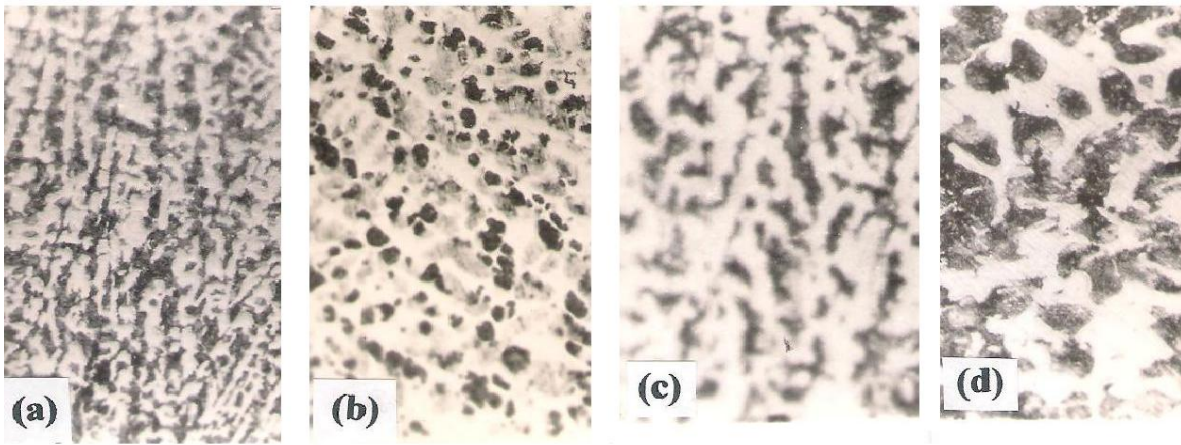


**Fig. 3:** Microstructure of skin layer of specimens with 1 wt % sulphur added to the molding sand for a)  $t = 10\text{mm}$ , b)  $t = 20\text{mm}$ , c)  $t = 30\text{mm}$ , and d)  $t = 40\text{mm}$  (100X).

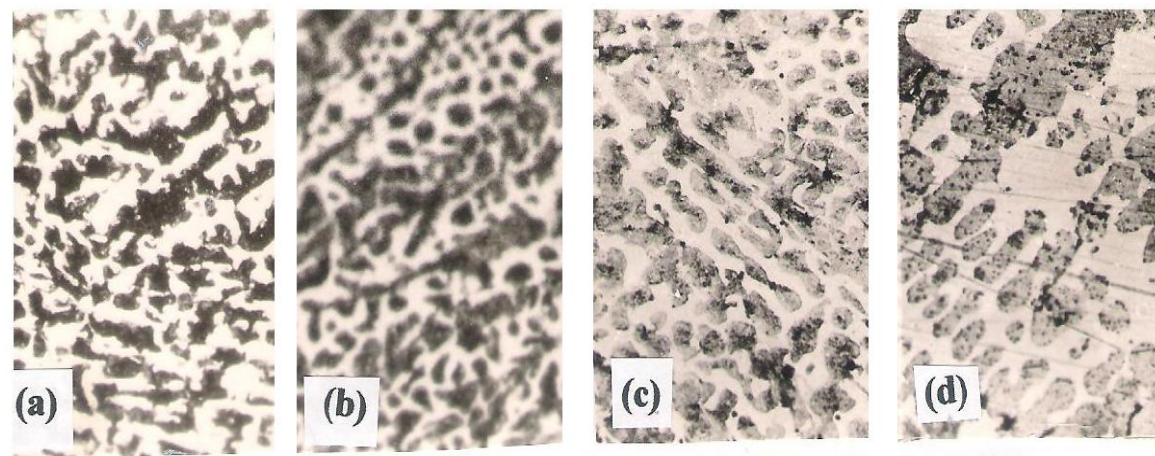


**Fig. 4:** Microstructure of skin layer of specimens with 2 wt % sulphur added to the molding sand for a)  $t = 10\text{ mm}$ , b)  $t = 20\text{ mm}$ , c)  $t = 30\text{ mm}$ , and d)  $t = 40\text{ mm}$  (100X).

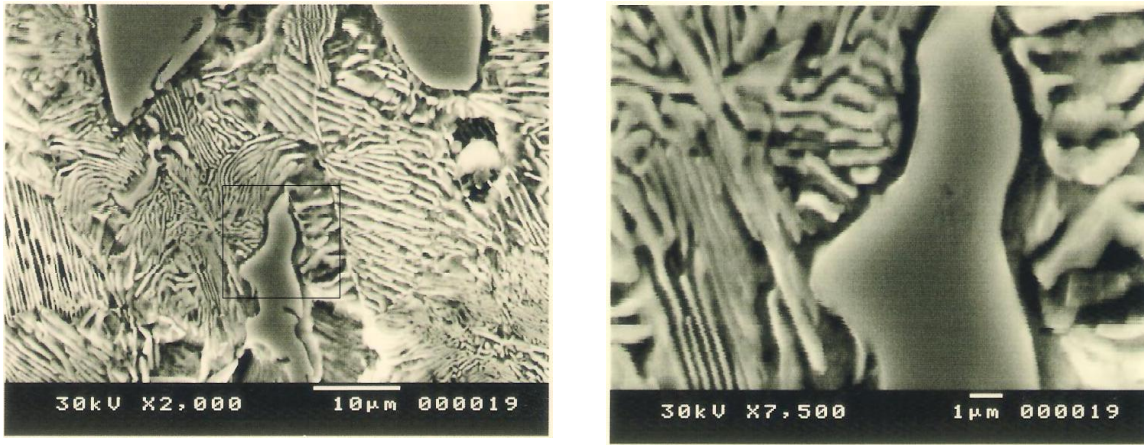


**Fig. 5:** Scanning electron micrograph of specimen with 2 wt% sulphur added to the moulding sand for thickness  $t = 10\text{mm}$  to show lamellar pearlite and cementite (proeutectoid + cementite) and ledeburite (pearlite + cementite).

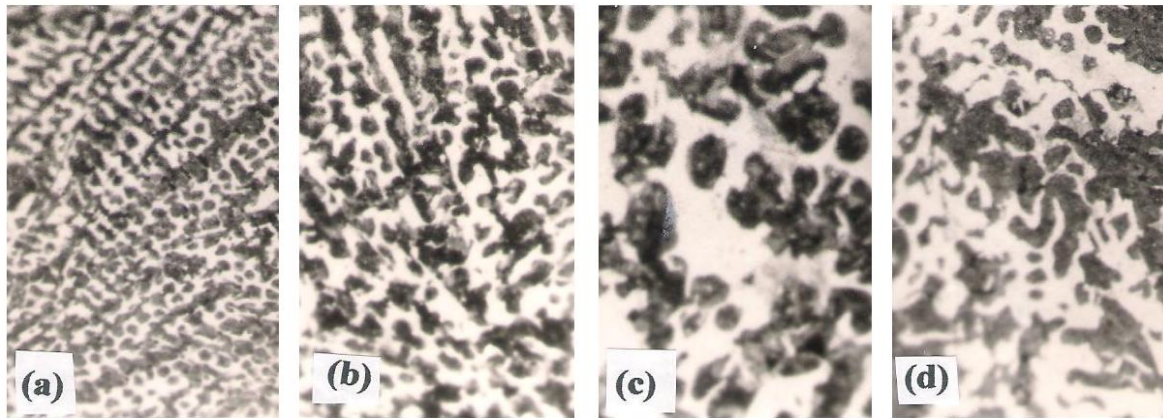


**Fig. 6:** Microstructure of skin layer of specimens with 4 wt. % sulphur added to the moulding sand for a)  $t = 10\text{ mm}$ , b)  $t = 20\text{ mm}$ , c)  $t = 30\text{ mm}$ , and d)  $t = 40\text{ mm}$  (100X).

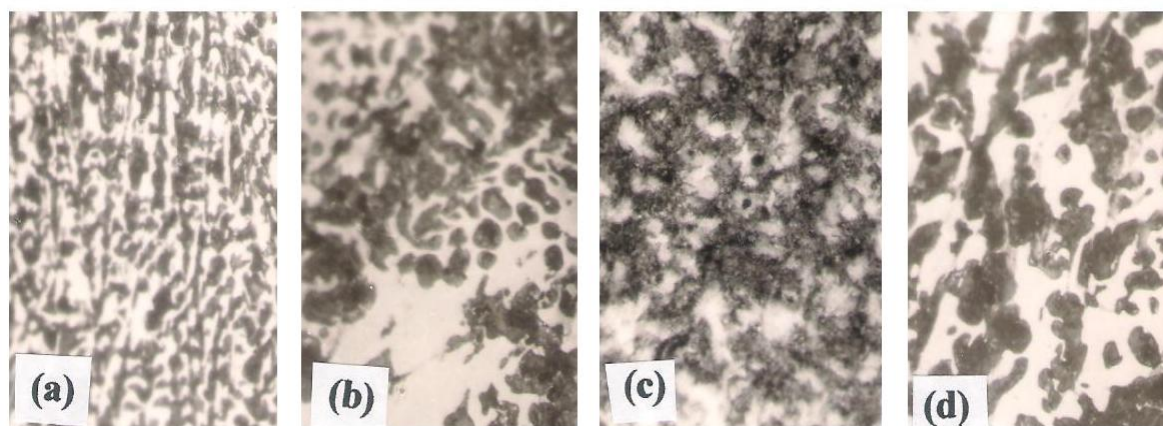


**Fig. 7:** Microstructure of skin layer of specimens with 6 wt. % sulphur added to the moulding sand for a)  $t = 10\text{ mm}$ , b)  $t = 20\text{ mm}$ , c)  $t = 30\text{ mm}$ , and d)  $t = 40\text{ mm}$  (100X).

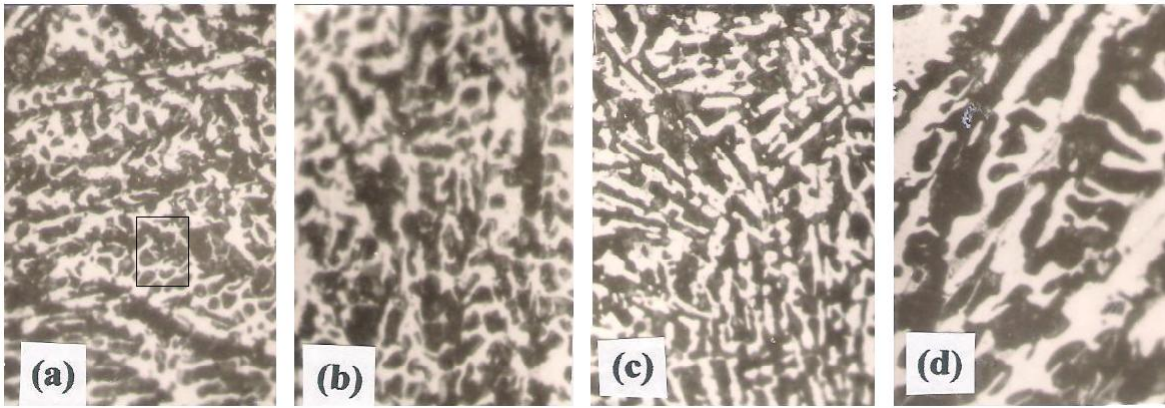


**Fig. 8: Microstructure of skin layer of specimens with 8 wt. % sulphur added to the molding sand for a)  $t = 10$  mm, b)  $t = 20$  mm, (c)  $t = 30$  mm, and d)  $t = 40$  mm (100X).**



**Fig. 9: The scanning electron micrograph of specimen with 8 wt.% sulphur added to the moulding sand for  $t = 10$  mm to show cementite (primary) and ledeburite .**

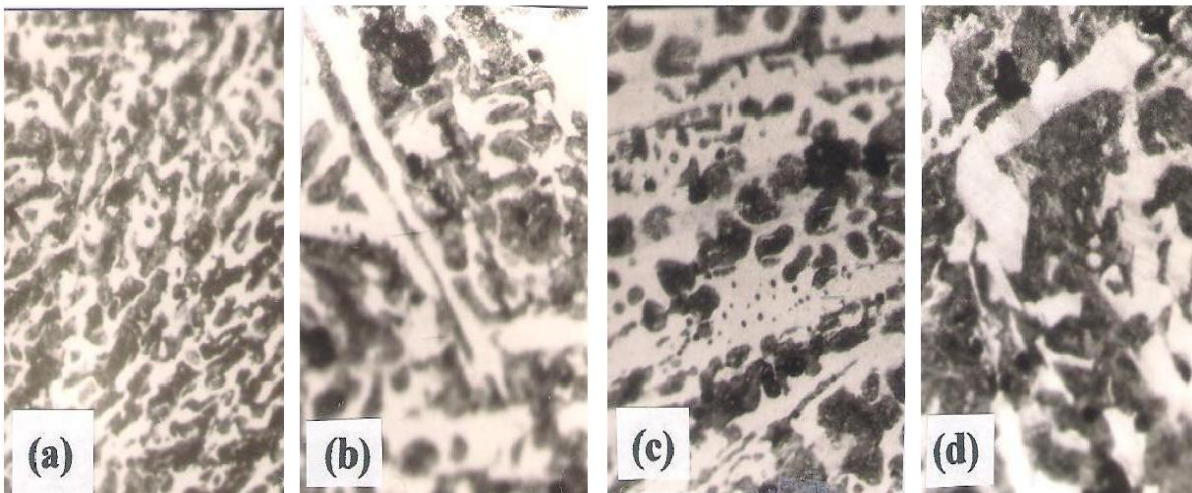


**Fig. 10: Microstructure of skin layer of specimens with 10 wt. % sulphur added to the molding sand for a)  $t = 10$  mm, b)  $t = 20$  mm, c)  $t = 30$  mm, and d)  $t = 40$  mm (100X).**

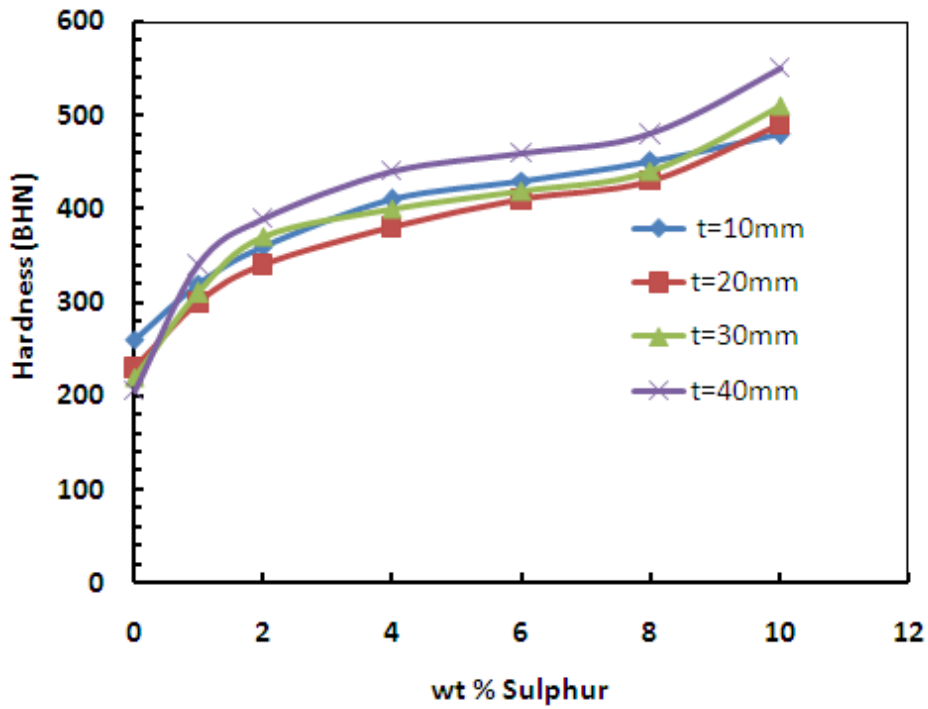


Fig. 11: Brinell hardness versus wt% sulphur additions on the molding sand of specimens for thicknesses 10 mm, 20 mm, 30 mm, 40 mm.

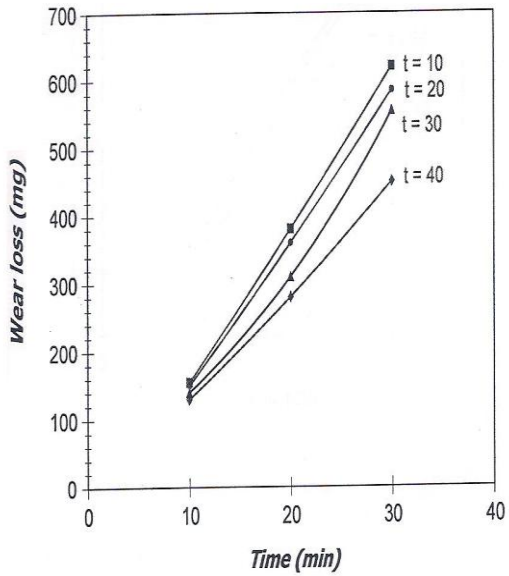


Fig. 12: Wear loss versus time for 0 wt% sulphur additions on the molding sand of specimens for thicknesses 10 mm, 20 mm, 30 mm and 40mm.

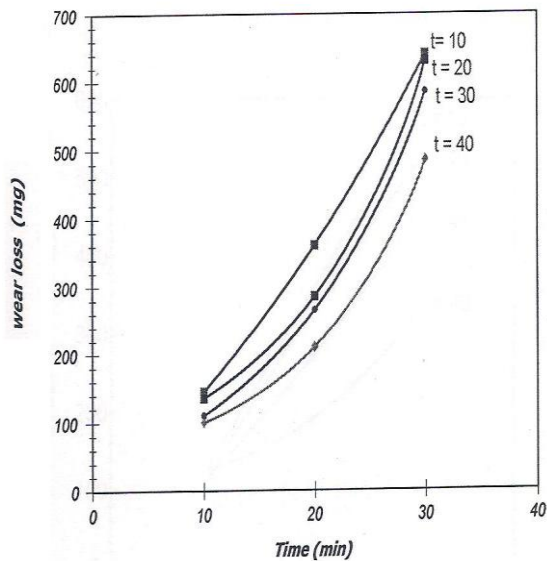
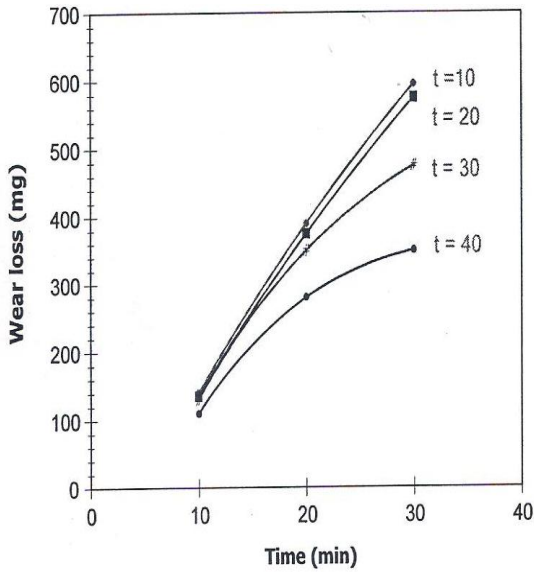
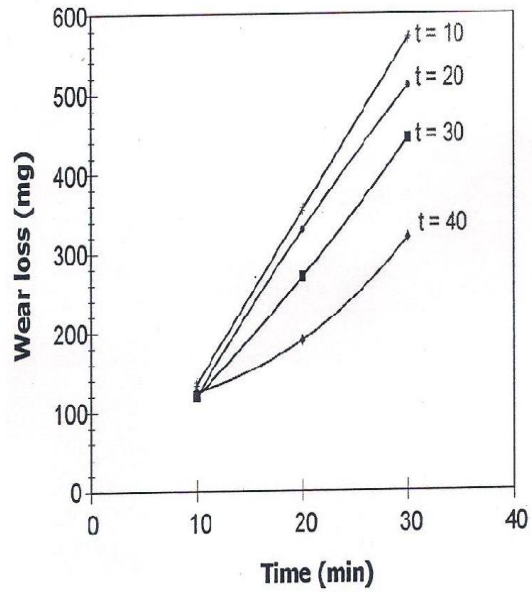


Fig. 13: Wear loss versus time for 1 wt% sulphur additions on the molding sand of specimens for thicknesses 10 mm, 20 mm, 30 mm and 40mm.



**Fig. 14:** Wear loss versus time for 2 wt.% sulphur additions on the molding sand of specimens for thicknesses 10 mm, 20 mm, 30 mm and 40 mm.



**Fig. 15:** Wear loss versus time for 4 wt.% sulphur additions on the molding sand of specimens for thicknesses 10 mm, 20 mm, 30 mm and 40 mm.

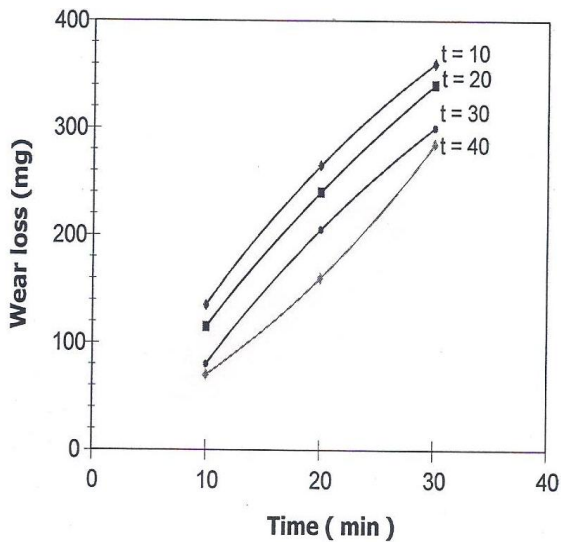


**Fig. 16:** Wear loss versus time of 6 wt.% sulphur additions on the molding sand of specimens for thicknesses 10 mm, 20 mm, 30 mm and 40 mm.

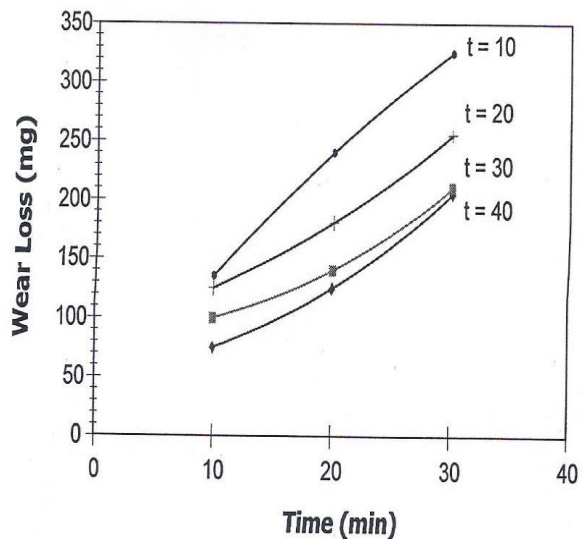


**Fig. 17:** Wear loss versus time of 8 wt.% sulphur additions on the molding sand of specimens for thicknesses 10 mm, 20 mm, 30 mm and 40 mm.

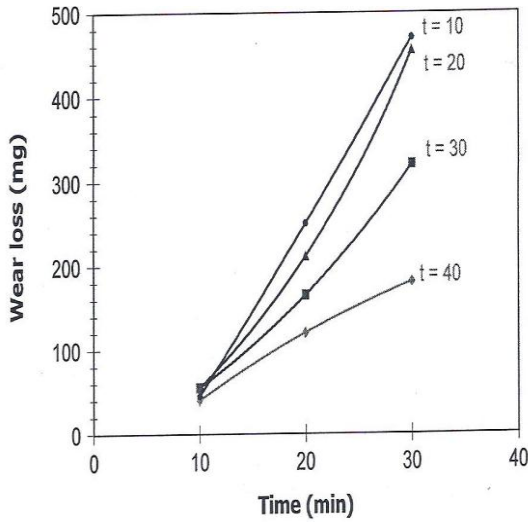


**Fig. 18:** Wear loss versus time for 10 wt.% sulphur additions on the molding sand of specimens of thicknesses 10 mm, 20 mm, 30 mm and 40 mm.

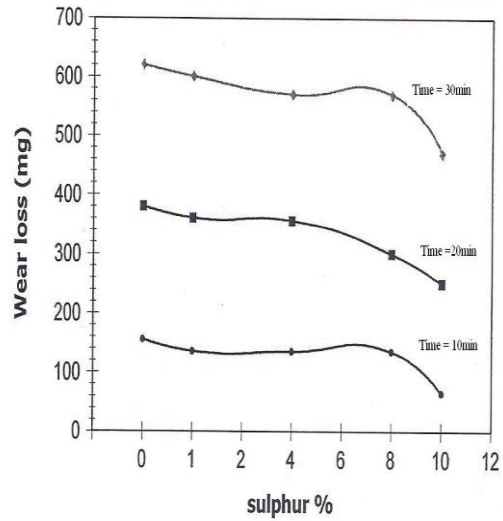


**Fig. 19:** Wear loss versus sulphur wt% additions on the molding sand of specimens for thickness  $t = 10$  mm with time 10, 20, and 30 min.

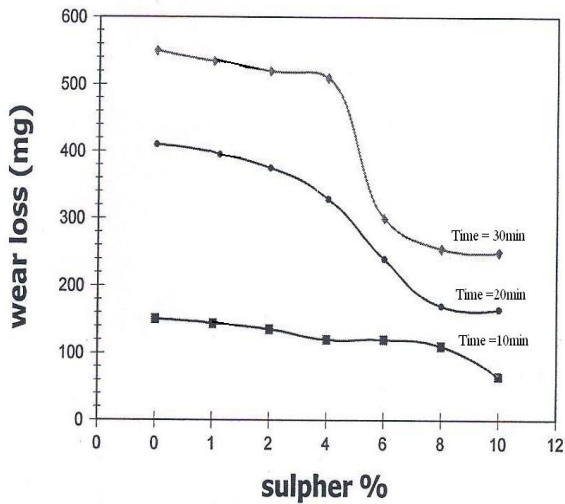


**Fig. 20:** Wear loss versus sulphur wt% additions on the molding sand of specimens for thickness  $t = 20$  mm with time 10, 20, and 30 min.

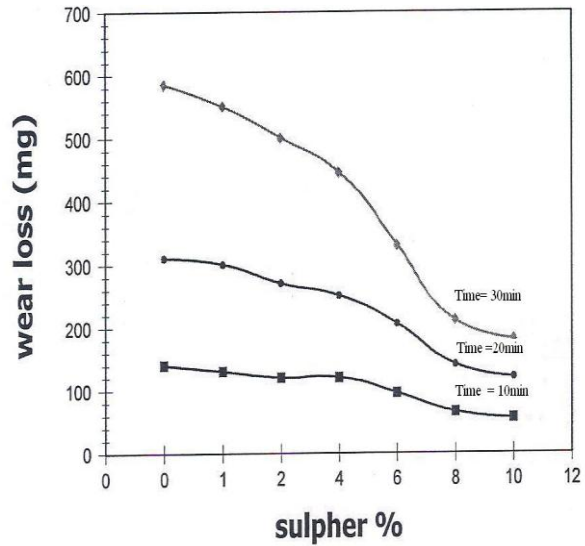


**Fig. 21:** Wear loss versus sulphur wt% additions on the molding sand of specimens of thickness  $t = 30$  mm with time 10, 20, and 30 min.

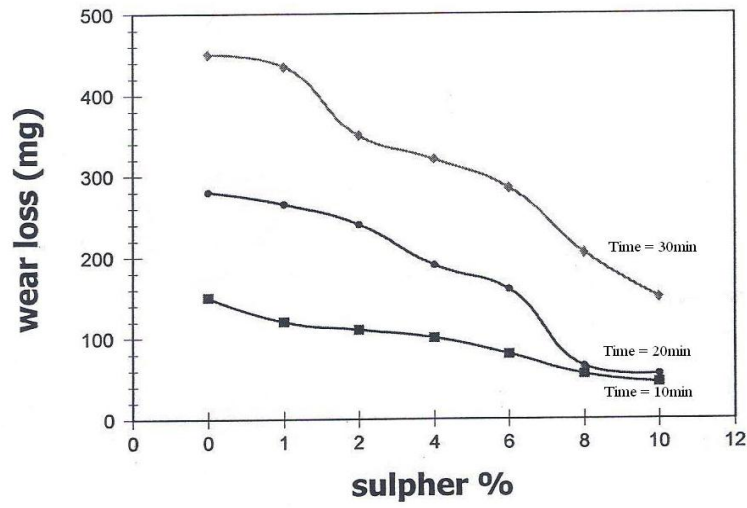


**Fig. 22: Wear loss versus sulphur wt% additions on the molding sand of specimens for thickness  $t = 40$  mm and time 10, 20, 30 min.**